LETTERS
PUBLISHED ONLINE: 21 NOVEMBER 2010 | DOI: 10.1038/NGEO1012

nature geoscience

Sea level as a stabilizing factor for marine-ice-sheet grounding lines

Natalya Gomez[1]*, Jerry X. Mitrovica[1], Peter Huybers[1] and Peter U. Clark[2]

Climate change could potentially destabilize marine ice sheets, which would affect projections of future sea-level rise[1-4]. Specifically, an instability mechanism[5-8] has been predicted for marine ice sheets such as the West Antarctic ice sheet that rest on reversed bed slopes, whereby ice-sheet thinning or rising sea level leads to irreversible retreat of the grounding line. However, existing analyses of this instability mechanism have not accounted for deformational and gravitational effects that lead to a sea-level fall at the margin of a rapidly shrinking ice sheet[9-11]. Here we present a suite of predictions of gravitationally self-consistent sea-level change following grounding-line migration. Our predictions vary the initial ice-sheet size and also consider the contribution to sea-level change from various subregions of the simulated ice sheet. Using these results, we revisit a canonical analysis of marine-ice-sheet stability[5] and demonstrate that gravity and deformation-induced sea-level changes local to the grounding line contribute a stabilizing influence on ice sheets grounded on reversed bed slopes. We conclude that accurate treatments of sea-level change should be incorporated into analyses of past and future marine-ice-sheet dynamics.

Weertman[5] derived the following equation governing the grounding-line position L of a simple, two-dimensional, marine-based, steady-state ice sheet (see Fig. 1a):

$$\beta L + D_o = G L^{2/9} \qquad (1)$$

where β and D_o are initial, pre-loaded values for the bed slope (positive values denote increasing depth in direction of ice flow), and the minimum depth of the bed, respectively. With suitable choices for the accumulation rate, flow parameters and so on, the constant G equals 22.7 $m^{7/9}$. Physically, the left-hand side of this equation represents sea level at the grounding line, $D(L)$, where the ice is at the critical flotation thickness. The right-hand side of the equation describes the ice thickness (in terms of an equivalent thickness of water) required so that accumulation of ice balances mass flux across the grounding line.

The solution of equation (1) for various parameter choices is illustrated in Fig. 1b. As an example, the case of $D_o = 200$ m and $\beta = 0$ leads to one steady-state solution (blue circle) and increasing β to 0.4 m km^{-1} yields two steady-state solutions (red, green circles). In the figure we adopt the terms 'unstable' or 'stable' following the arguments of Weertman[5] (see Supplementary Information). In general, if the slope of the curve describing sea level at the grounding line is greater than the slope of $GL^{2/9}$ at a point of intersection, the ice sheet is in a stable steady state; the ice sheet is unstable if the reverse is true. Whenever the initial bed slope, β, is less than or equal to zero, the solution is unconditionally

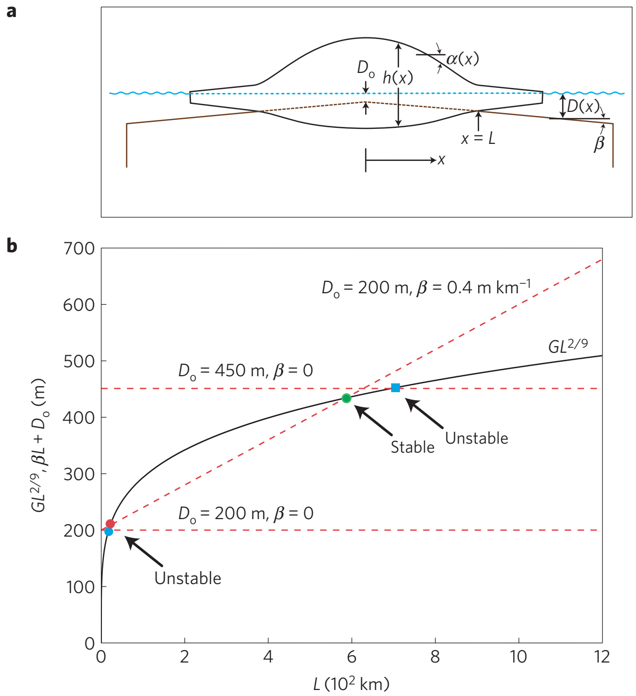

Figure 1 | A summary of the Weertman analysis of ice-sheet stability. **a**, Vertical cross-section through the two-dimensional, marine-based ice sheet considered by Weertman[5]. The radial dimension is denoted by x, where $x = L$ is the grounding line. The ice sheet of thickness $h(x)$ is in isostatic equilibrium and sits on bedrock initially inclined with slope β, where positive β denotes a bedrock depth that increases as one moves outwards. D_o denotes the pre-loaded depth of the bedrock at the centre of the ice sheet, and α is the slope of the upper ice surface. **b**, Plot of solutions for grounding-line position according to Weertman's[5] steady-state marine ice-sheet stability theory. The figure shows $GL^{2/9}$ versus grounding-line position L (black line) and $\beta L + D_o$ versus L for various D_o and β values (red lines, as labelled). The intersections between the $GL^{2/9}$ curve and the straight lines (denoted by red, green and blue circles and the blue square) are solutions to equation (1) and they therefore represent possible steady-state marine-ice-sheet configurations. The terms 'stable' and 'unstable' that appear on the figure are defined in the Supplementary Information and main text.

unstable, and a small retreat (advance) of the ice margin would lead to greater mass loss (gain) across the grounding line than accumulation and thus further retreat (advance). This result is the basis for Weertman's[5] conclusion that the model ice sheet is

[1]Department of Earth and Planetary Sciences, Harvard University, 20 Oxford Street, Cambridge, Massachusetts 02138, USA, [2]Department of Geosciences, Oregon State University, Corvallis, Oregon 97331, USA. *e-mail: ngomez@fas.harvard.edu.

inherently unstable when it rests on a bed that was flat or sloped downwards inland before loading.

One shortcoming of Weertman's[5] argument regarding stability is that it invokes a time-dependent perturbation of the system within an otherwise steady-state framework. For example, the bedrock topography is assumed to be in hydrostatic equilibrium with the ice load, even when the margin is advancing or retreating. Recent analyses have extended the Weertman treatment to account for, among other features, non-steady-state conditions[7,8,12]. These studies have indicated that the condition that an ice sheet on a reversed bed slope is unstable applies to the observed, rather than the pre-loaded, topography.

A second shortcoming of Weertman's analysis is the assumption that sea level at the grounding line remains constant as the size of the marine ice sheet is perturbed. Previous analyses have considered the influence of a sea-level perturbation (dD) on ice-sheet stability by assuming a geographically uniform, or eustatic, change in sea level[6,7,13,14]. The eustatic sea-level (ESL) change is simply the ratio of the volume of meltwater to the area of the oceans, and thus a decrease in ice mass, with an associated change in L, leads to an increase in sea level at the grounding line (Fig. 2a). The assumption of eustasy is roughly consistent with Weertman's assumption of hydrostatic equilibrium in the sense that adjustments in ice mass over very long timescales will maintain isostatic equilibrium and thus lead to sea-level changes that are nearly uniform geographically. However, isostatic equilibrium will not be maintained for ice-mass changes over timescales ranging out to tens of millennia, so that eustasy will generally be an inadequate description of changes in sea level, particularly near the ice sheet itself.

Gravitationally self-consistent sea-level (GSCSL) changes following rapid melting of grounded ice are, in fact, characterized by markedly non-uniform spatial patterns[9–11] (see Supplementary Information). The departure from eustasy is due to three effects: (1) elastic deformation of the solid Earth in response to the load redistribution, including a rebound of the crust in the vicinity of the diminishing ice load; (2) load self-gravitation, which primarily involves the migration of water away from the melting ice sheet as its gravitational pull on the ocean weakens; and (3) the feedback of contemporaneous, load-induced perturbations in the orientation of the Earth's rotation vector onto sea level. A GSCSL theory that combines these effects[11,15] (see the Methods section) predicts near-field sea-level changes in the opposite direction, and an order of magnitude larger, than would be predicted assuming eustasy (see Fig. 2a).

Consider an ice sheet with initial length $L_o = 700$ km that undergoes mass loss while maintaining a steady-state surface profile, consistent with the profile assumed by Weertman[5]. In this case, each kilometre of inward migration of the grounding line is associated with 0.30 m of sea-level fall (Fig. 2a). More generally, the predicted GSCSL change at the grounding line ranges from 0.20 to 0.34 m km^{-1} for grounding-line positions L ranging from 265 km to 1,400 km. This relative insensitivity occurs because the ice loss is largest at the margins and tapers off into the ice sheet and because the computed sea-level change at the grounding line is progressively less sensitive to ice-mass changes at greater distance.

This issue is explored in more detail in Fig. 2b,c, which shows the contribution to the GSCSL change from ice-mass changes within successively broader subregions of the ice-sheet-wide perturbation considered in Fig. 2a. In Fig. 2b, the sea-level change is plotted as a function of the fractional extent of ice-mass changes, as measured from the initial grounding line (see the caption). As an example, in the case $L_o = 700$ km, and mass changes confined to the outer 25% of the ice sheet, sea level changes by 0.24 m km^{-1}, or 80% of the ice-sheet-wide case. Figure 2c accounts for tapering of the ice loss from the margin to the interior by plotting the sea-level change as a function of the fractional cross-sectional area of the mass change, as measured from the initial grounding line. In the

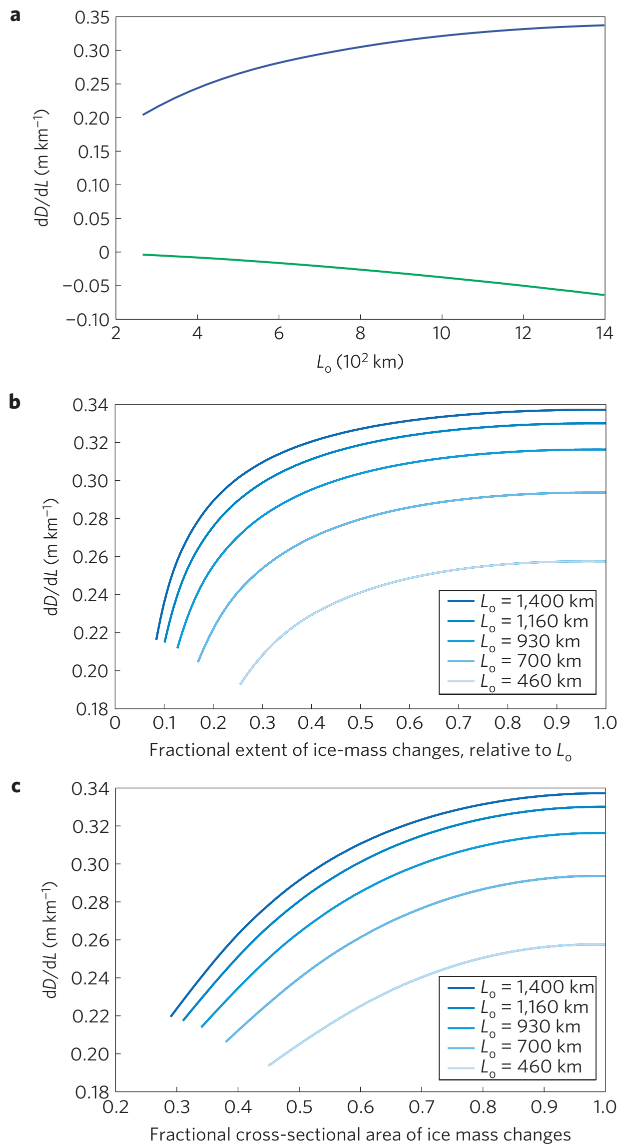

Figure 2 | Sea-level changes following grounding-line migration. **a**, Change in sea level at the grounding line divided by the change in the grounding-line position, that is, dD/dL, plotted as a function of the initial grounding-line position L_o. Green curve: A calculation that assumes a geographically uniform (eustatic) meltwater redistribution. Blue curve: A gravitationally self-consistent sea-level calculation (see the text and the Methods section). These calculations assume that the ice sheet maintains a steady-state surface profile as the grounding line migrates. **b**,**c**, Contributions to the GSCSL change (blue line in **a**), as a function of the fractional extent (**b**) or fractional cross-sectional area (**c**) of the total ice-load change in **a**. As an example, an x-axis value of 0.2 in **b** means that only mass change within a distance from the grounding line that is 20% of L_o is included. An x-axis value of 0.2 in **c** means that only 20% of the total cross-sectional area of melting in **a** that is closest to the grounding line is included.

$L_o = 700$ km case, for example, the 0.25 fractional extent that yields a sea-level change of 0.24 m km^{-1} corresponds to a fractional cross-sectional area of 0.5.

These sea-level results may be combined with the bed slope at the grounding line to compute an effective topographic slope. As an example, the grounding line of an ice sheet ($L_o = 700$ km) rapidly retreating on a flat bed will actually be subject to an effective topographic slope of 0.3 m km^{-1} (up towards the centre of the ice sheet) if the retreat reflects an ice-sheet-wide mass loss; this is as a result of the elastic uplift of the crust due to the (ice plus water) unloading and the fall of the local sea surface arising from the associated loss in gravitational attraction. Both processes act to stabilize the retreat of the grounding line.

Under what conditions would the sea-level feedback mechanism stabilize an ice sheet resting on a reversed bed slope? A preliminary answer to this question is possible by replacing, as we discussed above, the pre-loaded slope β in equation (1) with the observed slope, which we denote as β', and by adding an expression for the change in sea level that accompanies migration of the grounding line:

$$\beta' L + D_o + dD(L, dL) = GL^{2/9} \qquad (2)$$

Specifically, $dD(L, dL)$ is the change in sea level due to a shift of the grounding line from L to a new position, $L + dL$. For small changes in grounding-line position, δL, away from some reference value L_o, we can rewrite the additional term as

$$dD(L_o, \delta L) = \delta L \left.\frac{dD}{dL}\right|_{L=L_o}$$

We note that $\beta' + dD/dL$ represents the effective topographic slope at L_o, as defined above.

Figure 3 revisits the $D_o = 450$ km, flat-bed solution in Fig. 1 (blue square) using the extended stability equation (2). Under the assumption that the migration of the grounding line is accompanied by an ESL change, the instability we previously noted in the context of Fig. 1 is exacerbated. (That is, the slope of the green line is even lower than the slope of the black.) The inclusion of an ESL change perturbs the marine ice sheet towards a more unstable state. In contrast, if we incorporate a GSCSL change into the stability theory, a retreat of the grounding line from the original steady-state position ($L_o \sim 700$ km) will lead to a fall in sea level at the grounding line, a reduction of the flux across the grounding line and an advance of the ice sheet back to its original configuration. The marine ice sheet will thus be stable.

We conclude that local sea-level change following rapid grounding-line migration will contribute a stabilizing influence on marine ice sheets, even when grounded on beds of non-negligible reversed slopes, that is, $\beta' < 0$. In the Supplementary Information we use the results in Fig. 2 to explore the relationship between the magnitude of the stabilizing effect and the spatial scale of the ice-mass change (Supplementary Fig. S1). We demonstrate that the stabilization may be important even in the case of relatively localized perturbations in ice mass.

Note that the ice-mass perturbation need not be instantaneous. Our predictions of GSCSL change are based on elastic Earth models, and they are therefore accurate for mass changes integrated over timescales up to ~300–500 years (the Earth's Maxwell time). The issue of timescale is also relevant to our neglect of sea-level variations due to (meltwater-induced) perturbations in ocean dynamics. Global ocean simulations[16] that include freshwater hosing from Greenland into the North Atlantic suggest that static sea-level perturbations will dominate dynamic effects in most of the world ocean once melt volumes have reached ~20 cm of equivalent ESL change. In the near-field of the ice sheet, where the GSCSL changes are largest, this dominance will probably be established at much lower magnitudes of melt. We also note that changes in sea level associated with freshening or warming could be compensated for by a decrease in the density of water so that the flotation thickness of the ice at the grounding would be less affected.

We have highlighted the potential importance of the sea-level mechanism using a highly simplified model of marine ice-sheet stability based on that of Weertman[5]. More complete descriptions of grounding-line dynamics and marine-ice-sheet stability have

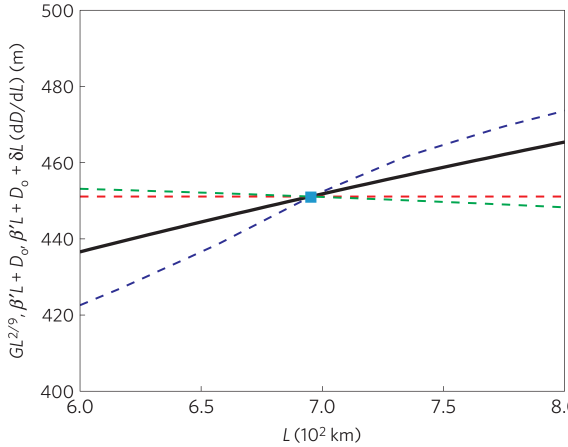

Figure 3 | Revised analysis of marine-ice-sheet stability based on a theory (equation (2)) that includes GSCSL change. The figure specifically considers the steady-state, flat-bed ice-sheet configuration denoted by the blue square ($D_o = 450$ km; $L_o \sim 700$ km) in Fig. 1b. The solid black and dashed red lines are reproduced from that figure. The dashed green and blue lines represent the total sea level at the grounding line computed by including either an ESL or GSCSL change (see the text or the Methods section), respectively, associated with a perturbation in ice-sheet size from the steady-state configuration (that is, the left-hand side of equation (2)). That is, we compute the term $dD(L_o, dL)$ as a function of the change in the grounding-line position, $dL = L - L_o$, away from the value L_o while maintaining a steady-state surface profile and add this to the red dashed line.

been developed that include ice-shelf buttressing[17,18], boundary layers to model the ice-sheet/ice-shelf transition zone[7,12] and an extension to three dimensions[8]. However, the GSCSL physics we have described is universal, and thus it will be active regardless of the level of complexity in the ice-sheet stability theory. In this regard, our results provide a framework for including the sea-level stabilization mechanism in more realistic models and, in turn, should lead to improved estimates of the stability and possible rates of change of marine-ice sheets such as the West Antarctic ice sheet.

Methods

We compute gravitationally self-consistent sea-level changes using a sea-level equation[11,15] valid for a one-dimensional (depth varying), elastic and rotating Earth model with time-varying shorelines. The predictions are generated using a pseudo-spectral sea-level algorithm[11,15,19] with truncation at spherical harmonic degree and order 512. (Values in Fig. 2 are calculated by reducing the grounding-line position by approximately 100 km, and computing the change in sea level at the new grounding line. Analogous values obtained using smaller changes in the grounding-line position will be progressively, but moderately, higher.) The elastic and density structure of the Earth model is prescribed by the seismic preliminary reference Earth model[20] (PREM), with this structure embedded in the elastic Love numbers[21].

Received 5 July 2010; accepted 13 October 2010; published online 21 November 2010

References

1. Oppenheimer, M. Global warming and the stability of the West Antarctic Ice Sheet. *Nature* **393,** 325–332 (1998).
2. Meehl, G. A. *et al.* in *IPCC Climate Change 2007: The Physical Science Basis: Contribution of Working Group I to the Fourth Assessment Report of the Intergovernmental Panel on Climate Change* (eds Solomon, S. *et al.*) 748–845 (Cambridge Univ. Press, 2007).
3. Vaughan, D. G. West Antarctic Ice Sheet collapse—the fall and rise of a paradigm. *Clim. Change* **91,** 65–79 (2008).
4. Smith, J. B. *et al.* Assessing dangerous climate change through an update of the Intergovernmental Panel on Climate Change (IPCC), 'reasons for concern'. *Proc. Natl Acad. Sci. USA* **106,** 4133–4137 (2009).
5. Weertman, J. Stability of the junction of an ice sheet and an ice shelf. *J. Glaciol.* **13,** 3–11 (1974).

6. Thomas, R. H. & Bentley, C. R. A model for Holocene retreat of the West Antarctic Ice Sheet. *Quat. Res.* **10,** 150–170 (1978).
7. Schoof, C. Ice sheet grounding line dynamics: Steady states, stability and hysteresis. *J. Geophys. Res.* **112,** F03S28 (2007).
8. Katz, R. F. & Worster, M. G. Stability of ice-sheet grounding lines. *Proc. R. Soc. A* **466,** 1597–1620 (2010).
9. Mitrovica, J. X., Tamisiea, M. E., Davis, J. L. & Milne, G. A. Recent mass balance of polar ice sheets inferred from patterns of global sea-level change. *Nature* **409,** 1026–1029 (2001).
10. Plag, H. P. & Jüttner, H-U. in *Proc. Second Int. Symp. on Environmental research in the Arctic and Fifth Ny-Ålesund Scientific Seminar* (ed. Yamanouchi, T.) No. 54 *Memoirs of the National Institute of Polar research* (Special Issue) 301–317 (2001).
11. Gomez, N., Mitrovica, J. X., Tamisiea, M. E. & Clark, P. U. A new projection of sea level change in response to collapse of marine sectors of the Antarctic Ice Sheet. *Geophys. J. Int.* **180,** 623–634 (2010).
12. Schoof, C. Marine ice-sheet dynamics. Part 1. The case of rapid sliding. *J. Fluid Mech.* **573,** 27–55 (2007).
13. Hindmarsh, R. & Le Meur, E. Dynamical processes involved in the retreat of marine ice-sheets. *J. Glaciol.* **47,** 271–282 (2001).
14. Wilchinsky, A. V. Linear stability analysis of an ice sheet interacting with the ocean. *J. Glaciol.* **55,** 13–20 (2009).
15. Kendall, R. A., Mitrovica, J. X. & Milne, G. A. On post-glacial sea level II. Numerical formulation and comparative results on spherically symmetric models. *Geophys. J. Int.* **161,** 679–706 (2005).
16. Kopp, R. E. *et al.* The impact of Greenland melt on local sea levels: A partially coupled analysis of dynamic and static equilibrium effects in idealized water-hosing experiments. *Clim. Change* doi:10.1007/s10584-010-9935-1 (2010, in the press).
17. Dupont, T. K. & Alley, R. B. Assessment of the importance of ice-shelf buttressing to ice-sheet flow. *Geophys. Res. Lett.* **32,** L04503 (2005).
18. Goldberg, D., Holland, D. M. & Schoof, C. Grounding line movement and ice shelf buttressing in marine ice sheets. *J. Geophys. Res.* **114,** F04026 (2009).
19. Mitrovica, J. X. & Peltier, W. R. On postglacial geoid subsidence over the equatorial oceans. *J. Geophys. Res.* **96,** 20053–20071 (1991).
20. Dziewonski, A. M. & Anderson, D. L. Preliminary reference Earth model (PREM). *Phys. Earth Planet. Inter.* **25,** 297–356 (1981).
21. Farrell, W. E. Deformation of the Earth by surface loads. *Rev. Geophys. Space Phys.* **10,** 761–797 (1972).

Acknowledgements

This research was financially supported by Harvard University, the Natural Sciences and Engineering Research Council of Canada (N.G.), the Canadian Institute for Advanced Research (J.X.M.), the Packard Foundation (P.H.) and the National Science Foundation (P.U.C.). We thank D. Pollard for comments that helped to improve this manuscript.

Author contributions

N.G. and J.X.M. were responsible for the sea-level modelling and all authors contributed to the modelling and discussion of ice-sheet stability and the writing and editing of the manuscript.

Additional information

The authors declare no competing financial interests. Supplementary information accompanies this paper on www.nature.com/naturegeoscience. Reprints and permissions information is available online at http://npg.nature.com/reprintsandpermissions. Correspondence and requests for materials should be addressed to N.G.